

5-2020

## Investigating the Effect of Hydrophilic Block Length on the Co-Assembly Behavior of Amphiphilic Triblock Copolymers

Alexandra M. Garrett

Follow this and additional works at: [https://aquila.usm.edu/honors\\_theses](https://aquila.usm.edu/honors_theses)



Part of the [Polymer Science Commons](#)

---

### Recommended Citation

Garrett, Alexandra M., "Investigating the Effect of Hydrophilic Block Length on the Co-Assembly Behavior of Amphiphilic Triblock Copolymers" (2020). *Honors Theses*. 713.

[https://aquila.usm.edu/honors\\_theses/713](https://aquila.usm.edu/honors_theses/713)

This Honors College Thesis is brought to you for free and open access by the Honors College at The Aquila Digital Community. It has been accepted for inclusion in Honors Theses by an authorized administrator of The Aquila Digital Community. For more information, please contact [Joshua.Cromwell@usm.edu](mailto:Joshua.Cromwell@usm.edu), [Jennie.Vance@usm.edu](mailto:Jennie.Vance@usm.edu).

The University of Southern Mississippi

Investigating the Effect of Hydrophilic Block Length on the Co-Assembly Behavior of  
Amphiphilic Triblock Copolymers

By

Alexandra Garrett

A Thesis

Submitted to the Honors College of

The University of Southern Mississippi

in Partial Fulfillment

of the Requirement for the Degree of Bachelor of Science

in the Department of Polymer Science and Engineering

May 2020



Approved by:

---

Yoan C. Simon, Ph.D., Thesis Adviser  
Professor of Polymer Science

---

Derek L. Patton, Ph.D., Director  
School of Polymer Science and  
Engineering

---

Ellen Weinauer, Ph.D., Dean  
Honors College

## Abstract

Polymer vesicles and micelles have been of interest in the scientific community for the past few decades due to potential biomedical applications in areas such as drug delivery, nanoreactors, and biosensing. Polymer vesicles and micelles are formed through the self-assembly of amphiphilic block copolymers. The objective of this project is to gain a better understanding of the influence of hydrophilic block copolymer length and composition in controlling the resulting morphologies from the co-assembly of triblock copolymers. First, a hydrophobic block composed of poly(methyl acrylate) was synthesized using reversible addition-fragmentation chain-transfer (RAFT) polymerization mediated by a difunctional chain-transfer agent. The block was then chain-extended with hydrophilic blocks of poly (acrylic acid) of 2 different lengths. The resulting two triblocks were then co-assembled at different ratios and the structure of the co-assemblies were characterized via light scattering.

**Keywords:** amphiphilic block triblock polymers, RAFT polymerization, self-assembly

## **Acknowledgements**

I would like to express my gratitude to my advisor Dr. Yoan Simon for his mentorship and guidance throughout my undergraduate research career. I would like to give a special thank you to my graduate mentor, Tamuka Chidanguro, for his patience and understanding during my research career at USM. They both taught me invaluable skills for working in a research lab. I would also like to give thanks to everyone in Simon research group for taking time to answer my questions and for creating a fun atmosphere. Thank you, Dr. Simon, for giving me the opportunity to gain skills that I will take with me for the rest of my career.

I would like to thank my parents and grandparents for giving me endless support and love throughout my time at USM. Without my parents' support and encouragement, I would not be the person I am today. I would also like to thank my friend David. He has given me boundless support and help through my four years at USM. I would have not been able to make this document without all the support I received throughout my time at USM.

## Table of Contents

List of Schemes .....	vii
List of Tables .....	viii
List of Figures.....	iv
List of Abbreviations .....	xi
Chapter 1: Introduction .....	1
1.1 Block copolymers .....	1
1.2 RAFT polymerization.....	3
1.3 Self- and Co- assembly of the different hydrophilic lengths .....	4
1.4 Characterization methods .....	6
1.5 Motivation.....	8
Chapter 2: Materials and Methods .....	10
2.1 Materials .....	10
2.2 Methods.....	10
2.2.1 Synthesis of Poly(methyl acrylate) (P(MA)).....	10
2.2.2 Chain extension of P(MA) with t-butyl acrylate (tBA) .....	11
2.2.3 Removal of t-butyl group to form acrylic acid (AA).....	11
2.2.4 Self- and co-assembly of the different hydrophilic lengths .....	12
2.2.5 Light Scattering .....	13
Chapter 3: Results and Discussion .....	14
3.1 Synthesis of P(MA) .....	14
3.2 Chain extension of P(MA) with tBA.....	15
3.3 Removal of t-butyl group .....	19
3.4 Self- and co-assembly of P78 and P328 .....	21
Chapter 4: Conclusion .....	27
Reference .....	28
Appendix.....	31

## List of Schemes

<b>Scheme 1.</b> Fundamental mechanisms of the common RDRPs. Dissociation-combination is typically done by NMP and some OMRP systems. Atom transfer is done by ATRP. Degenerate transfer are done by RAFT and some OMRP systems. <sup>10</sup> .....	2
<b>Scheme 2.</b> General mechanism for RAFT polymerization.....	3
<b>Scheme 3.</b> General structure for CTA. ....	4
<b>Scheme 4.</b> Synthesis of P(MA).....	14
<b>Scheme 5.</b> Chain extension of P(MA) with tBA for 1.25 hours and 3 hours to produce polymers with an $X_n$ of 79 and 328, respectively. ....	16
<b>Scheme 6.</b> Removal of t-butyl group through hydrolysis to form P(AA)- <i>b</i> -P(MA)- <i>b</i> -P(AA). ....	19

## List of Tables

<b>Table 1.</b> Light scattering data for the unfiltered samples .....	23
<b>Table 2.</b> Comparison of the hydrodynamic radius of the unfiltered and filtered samples.....	26

## List of Figures

<b>Figure 1.</b> Architectures of Block Terpolymers: Linear, Comb Graft Copolymers, Star and Cyclic Terpolymers. <sup>3</sup> .....	1
<b>Figure 2.</b> Morphologies from the assembly of amphiphilic polystyrene- <i>b</i> -poly(acrylic acid) (PS <sub><i>m</i></sub> - <i>b</i> -PAA <sub><i>n</i></sub> ) captured by transmission electron microscopy (TEM), where <i>m</i> and <i>n</i> are the degrees of polymerization of PS and PAA. <sup>2</sup> .....	5
<b>Figure 3.</b> Equipment set up for DLS. <sup>20</sup> .....	7
<b>Figure 4.</b> Equipment set up for SLS. <sup>22</sup> .....	8
<b>Figure 5.</b> Comparative NMR spectra for the synthesis of P(MA). From bottom to top, starting material, after reaction time, monomer removal under reduced pressure, final purification from monomer, and dried polymer.....	15
<b>Figure 6.</b> GPC (A) light scattering plot (B) differential refractive index plot of P(MA).....	15
<b>Figure 7.</b> Comparative NMR spectra of the extension P78. From bottom to top: comparing starting material, after reaction time, first purification, and dried polymer.....	16
<b>Figure 8.</b> GPC comparisons showing (A) light scattering (B) differential refractive index plots of the central P(MA) and the triblock polymer, P78.....	17
<b>Figure 9.</b> Comparative NMR spectra of the extension of P328. From bottom to top: starting material, after reaction time, first purification, and dried polymer.....	17
<b>Figure 10.</b> GPC comparison showing (A) light scattering (B) differential refractive index plots of the P(MA) central block to the triblock polymer, P328. ....	18
<b>Figure 11.</b> Comparative NMR spectra after <i>t</i> -butyl removal of P78. From bottom to top: starting material of P( <i>t</i> BA)- <i>b</i> -P(MA)- <i>b</i> -P( <i>t</i> BA), second hydrolysis, purification, and dried P(AA)- <i>b</i> -P(MA)- <i>b</i> -P(AA).....	20

**Figure 12.** Comparative NMR spectra after t-butyl removal from P328. From bottom to top: starting material of P(tBA)-*b*-P(MA)-*b*-P(tBA), second hydrolysis, purification, and P(AA)-*b*-P(MA)-*b*-P(AA)..... 21

**Figure 13.** Hydrodynamic diameter distribution curve of the morphologies obtained from the self-assembly of P78 triblock at 90° . ..... 22

**Figure 14.** Hydrodynamic diameter distribution curve of the morphologies obtained from P328 triblock at 90° ..... 22

**Figure 15.** Hydrodynamic diameter distribution curve of the morphologies obtained from the 25:75 (P78:328) mixture co-assembly 90° ..... 24

**Figure 16.** Hydrodynamic diameter distribution curve of the morphologies obtained from the 50:50 (P78:P328) mixture co-assembly 90° . ..... 24

**Figure 17.** Hydrodynamic diameter distribution curve of the morphologies obtained from the 75:25 (P78:P328) mixture co-assembly 90° . ..... 25

**Figure A-1.** The Zimm plot from the co-assembly of the 50:50 mixture of P78:P328..... 31

## List of Abbreviations

AA	acrylic acid
AIBN	4,4'-azobis(isobutyronitrile)
ATRP	atom transfer radical polymerization
CTA	chain-transfer agent
DCM	dichloromethane
DI	deionized
diCEP	di-4-cyano-4-(ethylsulfanylthiocarbonyl)sulfanylpentanoic acid
DLS	dynamic light scattering
DMF	<i>N,N</i> -dimethylformamide
GPC	gel permeation chromatography
MA	methyl acrylate
$M_n$	number-average molecular weight
NMP	nitroxide-mediated polymerization
NMR	nuclear magnetic resonance
OMRP	organometallic-mediated polymerizations
P(AA)	poly(acrylic acid)
P(MA)	poly(methyl acrylate)
P(tBA)	poly( <i>t</i> -butyl acrylate)

RAFT	reversible addition-fragmentation chain-transfer
RDRP	reversible-deactivation radical polymerization
SLS	static light scattering
$R_g$	radius of gyration
$R_h$	hydrodynamic radius
tBA	t-butyl acrylate
TEM	transmission electron microscopy
TFA	trifluoroacetic acid
THF	tetrahydrofuran
$X_n$	degree of polymerization

# Chapter 1

## Introduction

### 1.1 Block Copolymers

Block copolymers are composed of two or more polymer chains.<sup>1-3</sup> The blocks are covalently linked together and typically immiscible.<sup>2, 4</sup> Due to being immiscible the polymer will undergo microphase separation. Microphase separation will be further discussed later in this paper. Block copolymers can have various architectures. Common architectures types are linear diblock (AB), triblock (ABA), multiblock or segmented copolymer (AB)<sub>n</sub>, branch (graft and star) and cyclic molecular architectures.<sup>3, 5</sup> In Figure 1, some of the common architectures of block polymers are depicted. Reversible-deactivation radical polymerization (RDRP) is normally used to produce well-defined block copolymers.<sup>6</sup> This method allows for manipulation of polymer aspects such as weight distribution, composition, and architecture, while keeping the broad spectrum of possible monomers.

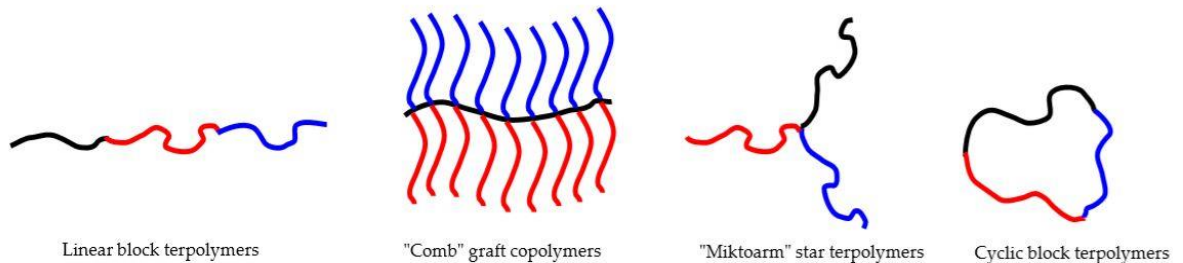
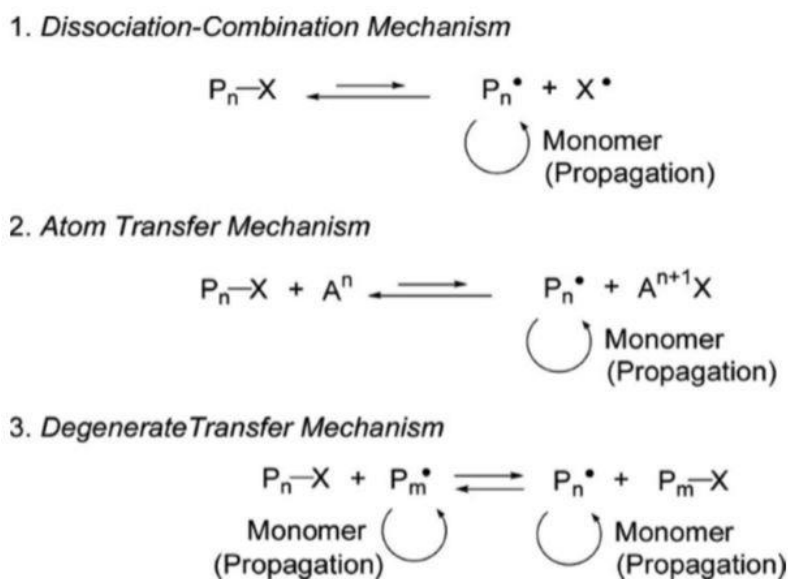


**Figure 1.** Architectures of Block Terpolymers: Linear, Comb Graft Copolymers, Star and Cyclic Terpolymers.<sup>3</sup>

RDRP was derived from living polymerization.<sup>7</sup> Living polymerization was first defined as a chain growth polymerization without transfer or termination.<sup>8</sup> Living polymerization method does not provide a control over the molecular weight or narrow molecular weight distributions.

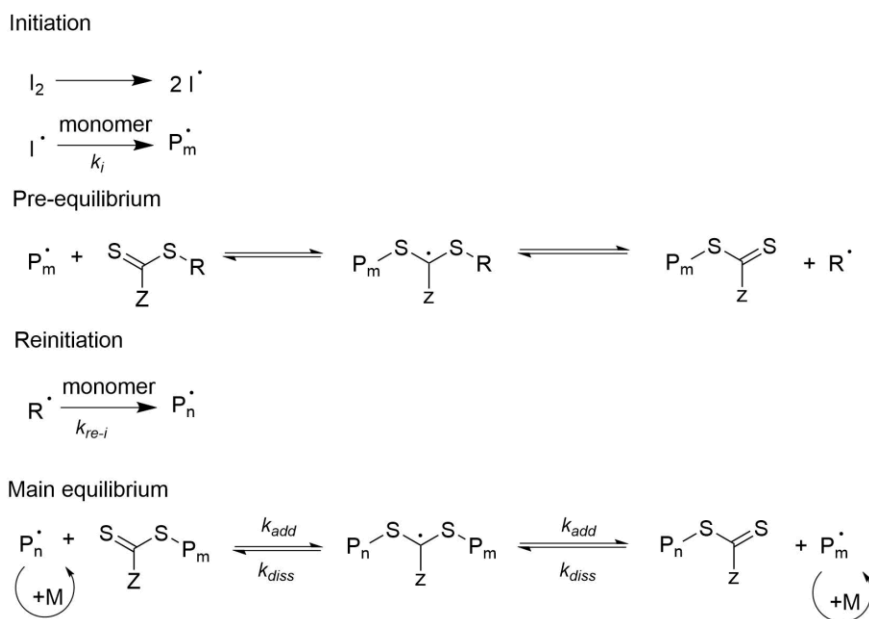
In order to achieve these goals, the initiator should be consumed at the early stages of the polymerization and the exchange between species of various activities is faster than the propagation step. Achieving these additional criteria, the polymerization is a controlled living polymerization. The investigation of adding radicals to unsaturated hydrocarbons laid the groundworks for RDRP methods.<sup>7</sup> The general principle of RDRP is reversible deactivation of living chain ends and rapid exchange between active and dormant chain ends to maintain a reactive polymer chain end. Four common polymerizations in this classification are nitroxide-mediated polymerization (NMP), atom transfer radical polymerization (ATRP), reversible addition-fragmentation chain-transfer (RAFT) polymerization, and organometallic-mediated polymerizations (OMRP).<sup>6,9</sup> Refer to Scheme 1 for fundamental mechanisms of the common RDRPs.



**Scheme 1.** Fundamental mechanisms of the common RDRPs. Dissociation-combination is typically done by NMP and some OMRP systems. Atom transfer is done by ATRP. Degenerate transfer are done by RAFT and some OMRP systems.<sup>9</sup>

## 1.2 RAFT polymerization

RAFT is a type of RDRP<sup>9</sup> and is one of the most versatile processes that allows for control of the reaction conditions and functionality.<sup>10</sup> This process allows for a wide range of monomers. RAFT has two main steps, initiation and propagation. There are two common types of initiators that are used for RAFT polymerization and they are peroxide and azo initiator.<sup>11</sup> During the initiation step, an initiator undergoes a homolytic cleavage. Then the radical initiator attacks the monomer to create oligomeric radicals.<sup>10</sup>



**Scheme 2.** General mechanism for RAFT polymerization.

Once the oligomeric radicals are formed, the radical will attack the chain-transfer agent (CTA) to form an intermediate as illustrated in the pre-equilibrium step modeled in Scheme 2.<sup>10</sup> A common type of CTA are thiocarbonylthio compound that bear an R and Z group.<sup>12</sup> In Scheme 3, illustrates the general structure of CTA. The reactivity of the R and Z group is significant when choosing a CTA.<sup>13</sup> The R group is the good leaving group that is better than the propagating radical but can still be used to initiate the polymerization.<sup>10</sup> The Z group affects the

kinetics of the polymerization to either stabilize or destabilize the CTA intermediate.<sup>13</sup> The R and Z group have demonstrated to influence the dispersity and the molecular weight of the polymer.<sup>10, 14</sup> Between the two groups, the Z group should be the primary focus when picking a CTA because the Z group affects the kinetics of the addition of monomers.<sup>11, 12, 14</sup> Some common Z group for CTAs are alkyl/phenyl (dithioesters), alkyl sulfides (trithiocarbonate), and alkoxides (xanthates).<sup>11</sup>



**Scheme 3.** General structure for CTA.

Once the intermediate is formed, the radical is moved to the R group to form an R group radical.<sup>10</sup> Reinitiation occurs when the monomer is added to the R group radical. The next step is propagation. The monomer is added to either the oligomeric radical or the R group radical for chain growth. This addition and alternation between the two radical species should be relatively fast to keep the concentration of growing chains lower than stable radical intermediates, which limits termination. Termination occurs either by combination or disproportionation. Once termination occurs, a second reaction can be set up with a different monomer to create a block polymer.

### ***1.3 Self-assembly of block copolymers in bulk and in solution***

Self-assembly of amphiphilic molecules has been an interest in the scientific community for the past few decades.<sup>2, 10</sup> In nature, the cell is one of the best examples that showcases this self-assembly process.<sup>22</sup> The cell has a phospholipid bilayer membrane which is formed through

self-assembly of amphiphilic phospholipids consisting of a hydrophobic tail and a hydrophilic head.

The self-assembly can be achieved in bulk or aqueous solution.<sup>2</sup> The self-assembly process in bulk is driven by an unfavorable mixing enthalpy with a small mixing entropy.<sup>2, 3</sup> The unfavorable mixing is brought on by thermodynamic incompatibility between the blocks which causes microphase separation.<sup>15</sup> Macrophase separation is prevented due to the blocks being covalently bonded. Different morphologies that can be achieved are spheres, cylinders, gyroids, and lamellae which is depicted in Figure 2.<sup>3</sup> There are three important parameters that affect the morphologies: the composition of the block copolymer, the number of repeating units, and the Flory-Huggins interaction parameter.

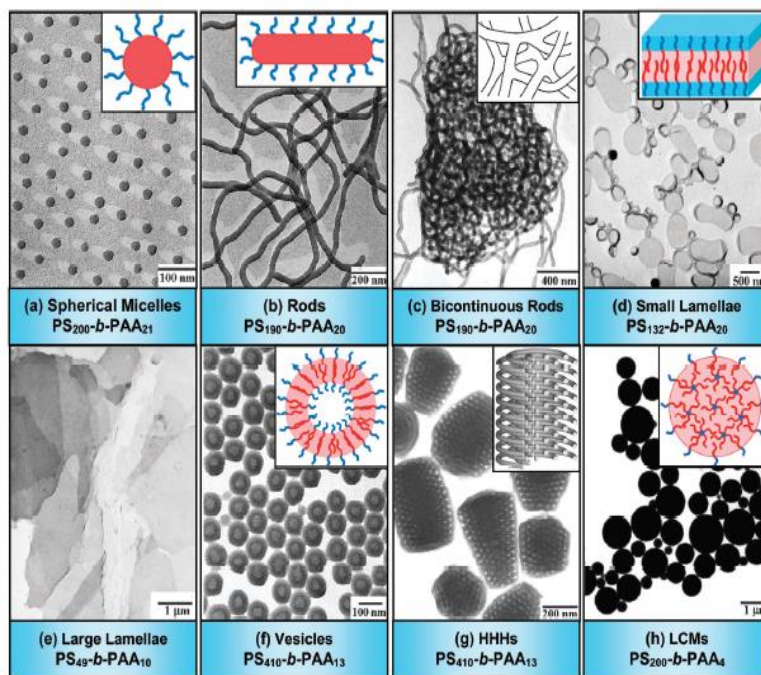


**Figure 2.** Morphologies from the assembly of amphiphilic polystyrene-*b*-poly(acrylic acid) ( $PS_m$ -*b*- $PAA_n$ ) captured by transmission electron microscopy (TEM), where *m* and *n* are the degrees of polymerization of PS and PAA.<sup>2</sup>

Performing self-assembly in solution increases the level of complexity because of the introduction of solvent.<sup>2</sup> Self-assembly in aqueous solution is driven by minimization of free energy in the system.<sup>3</sup> The general method for self-assembly in solution is to first dissolve the polymer in a good solvent for all the blocks.<sup>2</sup> Then a selective solvent, usually water, is slowly added to the solution until the water content is higher than when aggregation starts. Lastly, to freeze the kinetic process and morphology, excess water is added to the solution.

Morphology is primarily affected by the packing of the copolymer chains.<sup>16</sup> The packing parameter ( $p$ ) can be defined as:

$$p = \frac{v}{a_o l_c}$$

where  $v$  is the volume of the hydrophobic chains,  $a_o$  is the optimal area of the head group, and  $l_c$  is the length of the hydrophobic tail.<sup>16</sup> The packing parameter values suggest the morphology of the self-assembled polymer. When  $p \leq 1/3$ , a spherical micelle is favored. When  $1/3 \leq p \leq 1/2$ , cylindrical micelles are favored and when  $1/2 \leq p \leq 1$ , a vesicle is favored. Factors that can change the packing parameter are changing the block copolymer composition and concentration, water content, common solvent, and additives.<sup>3</sup>

#### ***1.4 Characterization methods***

Light scattering is a characterization method that is used to determine particle size, particle size distribution, and molecular weight.<sup>17,18</sup> When the light strikes a particle, it causes electrons around the particle to oscillate with the same energy as the light.<sup>19</sup> The oscillating electrons create an oscillating dipole in the particle. The oscillating dipole is the source of energy to scatter the light. Particles of different sizes will scatter with different intensities depending on the scattering angle. Some factors that affect the scattering of light are particle size, wavelength

dependence, the distance of the observed scattering of light, concentration, and molecular weight of the particles. Two conventional methods of light scattering are dynamic light scattering (DLS) and static light scattering (SLS). The principle of DLS is that the particles are hit with a monochromatic light that will generate scattered light waves in all directions.<sup>18</sup> The intensity of the scattered light is then measured at a known angle by a photon detector. Using DLS the hydrodynamic radius can be calculated using the Stokes-Einstein equation:

$$R = \frac{kT}{6\pi\eta D}$$

where  $k$  is the Boltzmann constant,  $T$  is the temperature in Kelvin,  $D$  is the diffusion coefficient, and  $\eta$  is the viscosity of the suspending medium. The Stokes-Einstein equation can only be used when there is a single scattered light, and the concentration of the sample is not too high. DLS is commonly used to analyze size distribution.

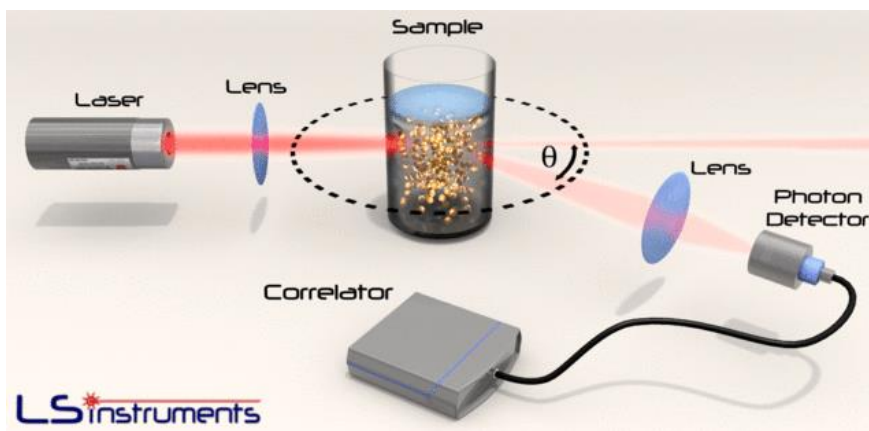


**Figure 3.** Equipment set up for DLS.

The principle of SLS is similar to DLS, with the exception that the intensity of the scattered light is measured at multiple known angles by a photon detector instead of just one angle.<sup>20</sup> The radius of gyration can be obtained from SLS by creating a Zimm plot. The radius of

gyration is used to determine the shape and size of the particle. Figure 2 and 3 are diagrams of the equipment set up for collecting experiment data for DLS and SLS.

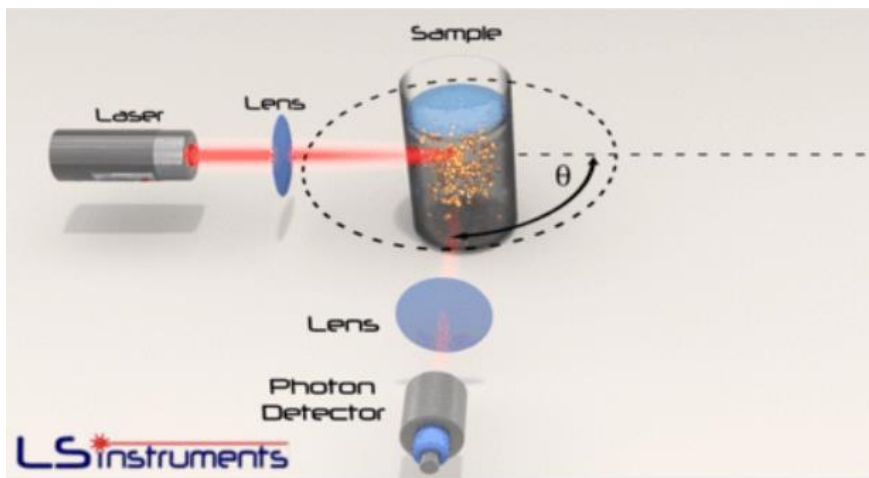


**Figure 4.** Equipment set up for SLS.<sup>21</sup>

In this project, the light scattering is used to monitor the hydrodynamic radius ( $R_h$ ), radius of gyration ( $R_g$ ), and distribution size. The ratio of  $R_g/R_h$  can be used to determine the morphology of the co-assembled polymer.<sup>17</sup> A micelle structure would be expected when the  $R_g/R_h$  ratio is less than one and a cylindrical micelle would be expected when  $R_g/R_h$  ratio is greater than one. A vesicle structure is expected to form with a  $R_g/R_h$  ratio of one.

### **1.5 Motivation**

The objective of this project is to have a better understanding of how we can control the morphology of the co-assembled triblock copolymers. The importance of this research is to further understand how to control the morphology of a self-assembled polymer to tailor them for biomedical applications such as drug delivery, nanoreactors, biosensing and gene therapy.<sup>2, 22</sup> In this project, amphiphilic triblock copolymers were synthesized using reversible addition-fragmentation chain-transfer (RAFT) polymerization. The hydrophobic block is comprised of poly(methyl acrylate) and the hydrophilic block is comprised of poly(acrylic acid). One polymer

will have a higher percent composition of the hydrophilic block (P328) while the other polymer will have a lower percentage (P78). The two triblock copolymers will be co-assembled at different ratios and the resulting self-assembled structures that will be characterized by light scattering.

*Research Question(s):*

1. How does the initial ratio of the two triblocks affect the morphology formed from co-assembly?

## Chapter 2

### Materials and Methods

#### 2.1 Materials

Dichloromethane (DCM) (Fisher Scientific; 99.9%), Hexanes (Fisher Scientific; 98.5%), N,N-Dimethylformamide (DMF) (Fisher Scientific; 99%), methanol (Fisher Scientific; 99.8%), tetrahydrofuran (THF) (Fisher Scientific; 99.8%), petroleum ether (Fisher Scientific; certified ACS), and trifluoroacetic acid (TFA) (Sigma-Aldrich; 99%) were used as received. Methyl acrylate (MA) (Alfa Aesar; 99%,) was filtered through basic alumina and t-butyl acrylate (tBA) (Alfa Aesar; 98%,) was filtered through neutral alumina. 4,4'-azobis(isobutyronitrile) (AIBN) (Sigma-Aldrich;98%) was recrystallized in cold methanol.

#### 2.2 Methods

##### 2.2.1 Synthesis of Poly(methyl acrylate) (P(MA))

A 20 mL reaction vial was charged with AIBN (6 mg, 0.037 mmol, 0.2 equiv.), di-4-cyano-4-(ethylsulfanylthiocarbonyl)sulfanylpentanoic acid (diCEP) (0.1 g, 0.181 mmol, 1 equiv.), and MA (7 g, 81.31 mmol, 449.48 equiv.). The vial was sealed and purged with argon at 0°C for 15 minutes. The solution was then placed in an oil bath set at 80°C for 6 hours. The reaction was stopped by exposing the solution to air and quenching in liquid nitrogen. The target molecular weight was 20,000 g/mol at 50% conversion. The crude product was dissolved in DCM and precipitated out in hexanes. The polymer was dried in a vacuum oven overnight at room temperature to produce a yellow solid. <sup>1</sup>H NMR (300 MHz, CDCl<sub>3</sub>, δ, ppm): 3.67 (s, 3H), 2.44-2.22 (br, 2H), 2.04-1.38 (br, 2H).

### **2.2.2 Chain extension of P(MA) with *t*-butyl acrylate (tBA)**

A 20 mL reaction vial was charged with 0.4 g of P(MA) (0.022 mmol, 1 equiv.). In a separate vial, 5 mg of AIBN was dissolved in 2 mL of dry DMF. A separate vial was charged with 0.6 g of tBA (4.68 mmol, 214.4 equiv.). All the tBA was transferred to the reaction vial that contained P(MA). The vial that contained tBA was washed with 0.7 mL of dry DMF and transferred to the reaction vial. AIBN (0.3 mL, 0.005 mmol, 0.2 equiv.) was transferred to the reaction vial. The vial was sealed and purged with argon at 0°C for 15 minutes. The solution was then placed in an oil bath that was set at 80°C for 1.25 hours. The reaction was stopped by exposing the solution to air and quenching in liquid nitrogen. The target conversion was 30%, where the hydrophilic block is 30% of the overall composition. The polymer was dissolved in DCM and precipitated out in a 70:30 mixture of cold methanol and water. The polymer was dried in a vacuum oven at 35°C overnight to produce a pale-yellow solid.

A second polymerization was carried out with the same procedures but used 0.4 g of P(MA) (0.022 mmol, 1 equiv.), 5 mg of AIBN (0.005 mmol, 0.2 equiv.), 0.8 g of tBA (6.24 mmol, 285.9 equiv.). The reaction was stopped after 3 hours. The target was 70% conversion, where the hydrophilic block is 70% of the overall composition. <sup>1</sup>H NMR (300 MHz, CDCl<sub>3</sub>, δ, ppm) 3.67 (s, 3H), 2.73-2.49 (br, 2H), 2.42-1.61 (br, 2H), 1.44 (s, 3H).

### **2.2.3 Removal of *t*-butyl group to form acrylic acid (AA)**

The general procedure for the removal of the *t*-butyl group is as follows: dissolved the triblock polymer, P(tBA)-*b*-P(MA)-*b*-P(tBA), with DCM in a two-necked 100 mL round bottom flask. Stir the solution for 10 minutes. Add TFA (5 equiv.) and let the mixture stir for 12 hours at room temperature. The solvent was removed under pressure. The polymer was further purified

by dissolving it in THF and precipitating it out twice in petroleum ether. The polymer was dried in a vacuum oven overnight at room temperature to produce a yellow white solid. <sup>1</sup>H NMR (300 MHz, CDCl<sub>3</sub>, δ, ppm) 3.67 (s, 3H), 2.73-2.49 (br, 2H), 2.42-1.61 (br, 2H).

#### ***2.2.4 Self- and Co-assembly of the different hydrophilic lengths***

The self-assembly of the polymer with the target of 30% hydrophilic composition proceeded as follows: 10 mg of the triblock polymer was dissolved in 1 mL of THF for 30 minutes. Deionized (DI) water (3 mL) was added at 1mL/hour. This procedure was repeated for the polymer with the target of 70% hydrophilic composition.

The general procedure for the co-assembly of the polymer with the target of 30% hydrophilic composition and the polymer with the target of 70 % hydrophilic composition is as follows: a total of 10 mg of the polymers were dissolved in 1 mL of THF for 30 minutes. DI water (3 mL) was added to the solution at 1 mL/hour. The ratios used for co-assembly are 25:75 (polymer with the target of 30% hydrophilic composition to polymer with the target of 70% hydrophilic composition), 50:50, and 75:25. For the 25:75 mixture, 2.5 mg of the polymer with the target of 30% hydrophilic composition and 7.5 mg of the polymer with the target of 70% hydrophilic composition were used. For the 50:50 mixture, 5 mg of both polymers were used. For the 75:25 mixture, 7.5 mg of the polymer with the target of 30% hydrophilic composition and 2.5 mg of the polymer with the target of 70% hydrophilic composition were used. The samples then underwent dialysis for 24 hours in DI water to remove THF in order to prepare them for analysis.

### 2.2.5 Light Scattering

Approximately 1 mL of each sample was transferred to a 12 x 75 mm tube. Then approximately 1 mL more of each sample was filtered with a 1.2  $\mu\text{L}$  filter before being transferred into a 12 x 75 mm tube.

Dynamic and static light scattering data were collected at 25°C. The time-dependent scattering intensities were measured with a Brookhaven Instruments BI-200SM goniometer that was equipped with an avalanche photodiode detector and TurboCorr correlator. The incident light used was 633 nm from a Research Electro Optics HeNe laser operating at 40 mW. The time-dependent scattering intensities were measured at 45, 60, 75, 90, 105, and 120° for DLS. In SLS the angles measured for the time-dependent scattering intensities were 45, 50, 60, 70, 80, 90, 105, 115, 120, and 140°.

To calculate the  $R_h$  values of the assembled polymers, the apparent diffusion coefficient needs to be calculated experimentally. The apparent diffusion coefficient is the slope of  $\Gamma$  versus  $q^2$ , where  $q$  is the wave vector and  $\Gamma$  is the relaxation frequency. The wave vector is calculated using the following equation:

$$q = \frac{4\pi n}{\lambda} \sin\left(\frac{\theta}{2}\right)$$

Where  $\lambda$  is the wavelength of the incident light,  $\theta$  is the scattering angle, and  $n$  is the refractive index of the solvent. The relaxation frequency was obtained from the quadratic fit of the autocorrelation function ( $g^2(\tau)$ ),

$$\Gamma = \tau^{-1}$$

where  $\tau$  is the relaxation time. With the apparent diffusion coefficient of the assembled samples, the  $R_h$  can be calculated using the Stokes-Einstein equation.



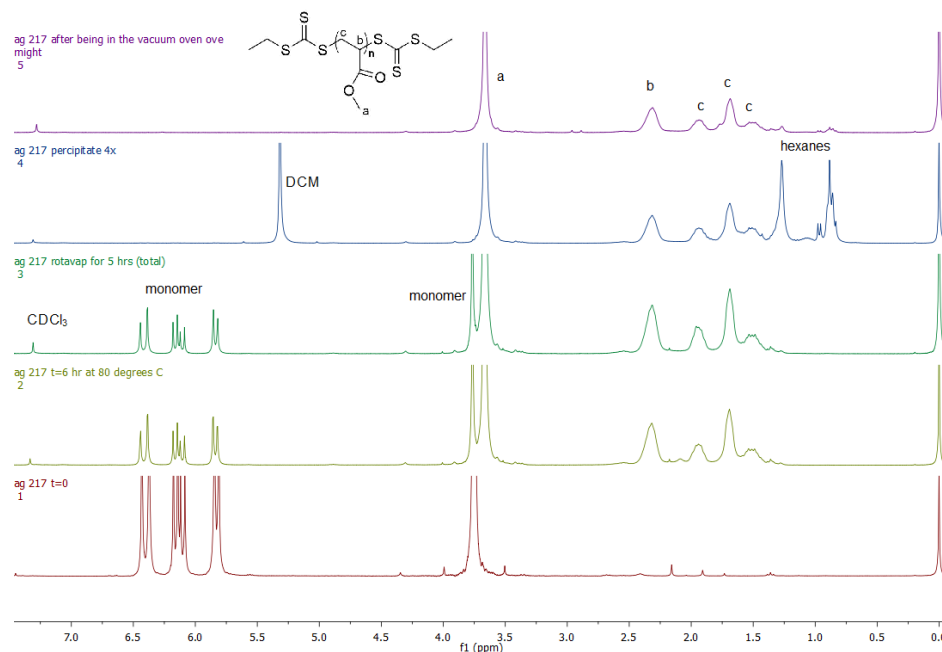


**Figure 5.** Comparative NMR spectra for the synthesis of P(MA). From bottom to top: starting material, after reaction time, monomer removal under reduced pressure, final purification from monomer, and dried polymer.

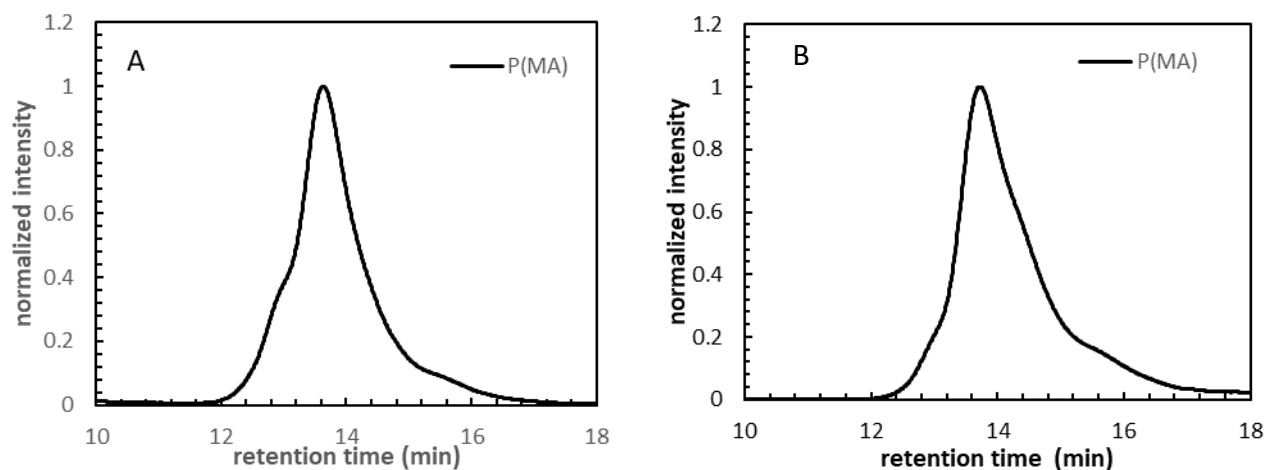
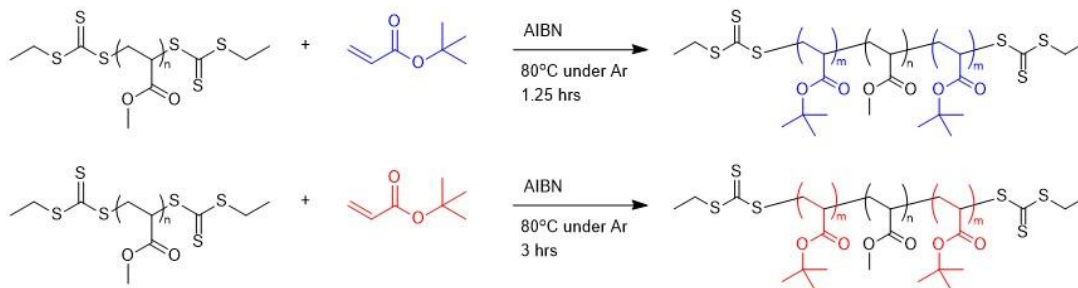


**Figure 6.** GPC (A) light scattering plot (B) differential refractive index plot of P(MA).

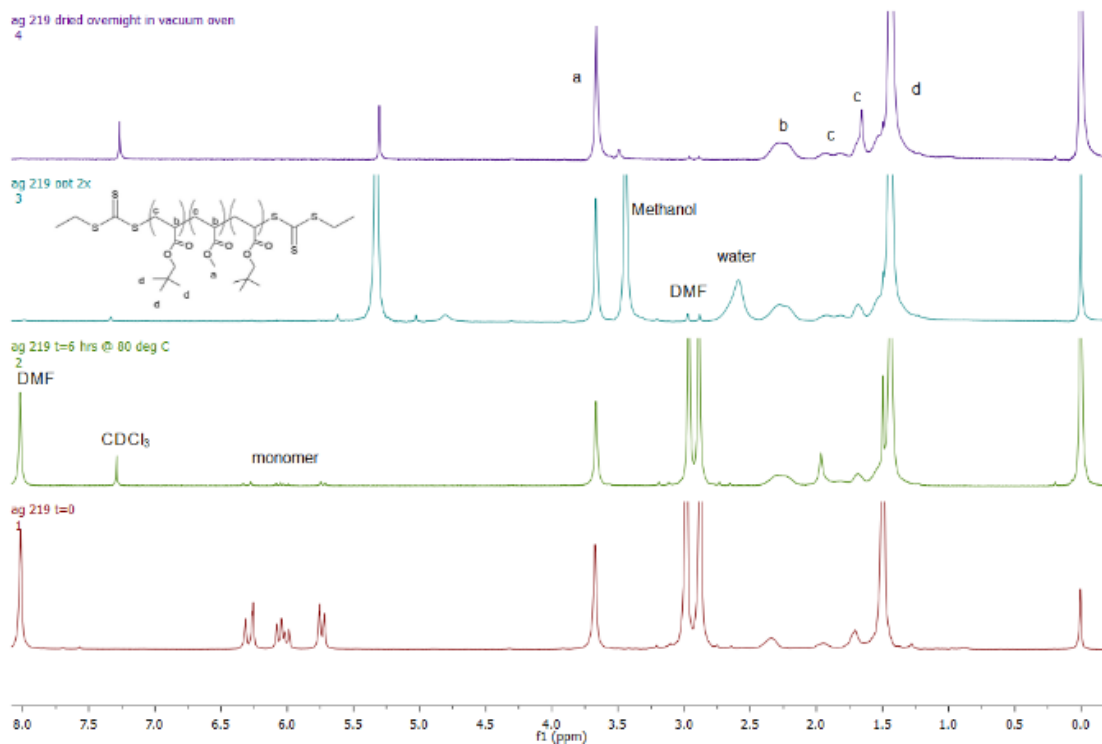
### 3.2 Chain extension of P(MA) with tBA

The P(MA) chain was then extended with tBA via RAFT polymerization to form an ABA triblock copolymer. The extension was performed twice to synthesize two polymers with different hydrophilic block lengths as illustrated in Scheme 5. The  $^1\text{H}$  NMR spectra on Figure 7

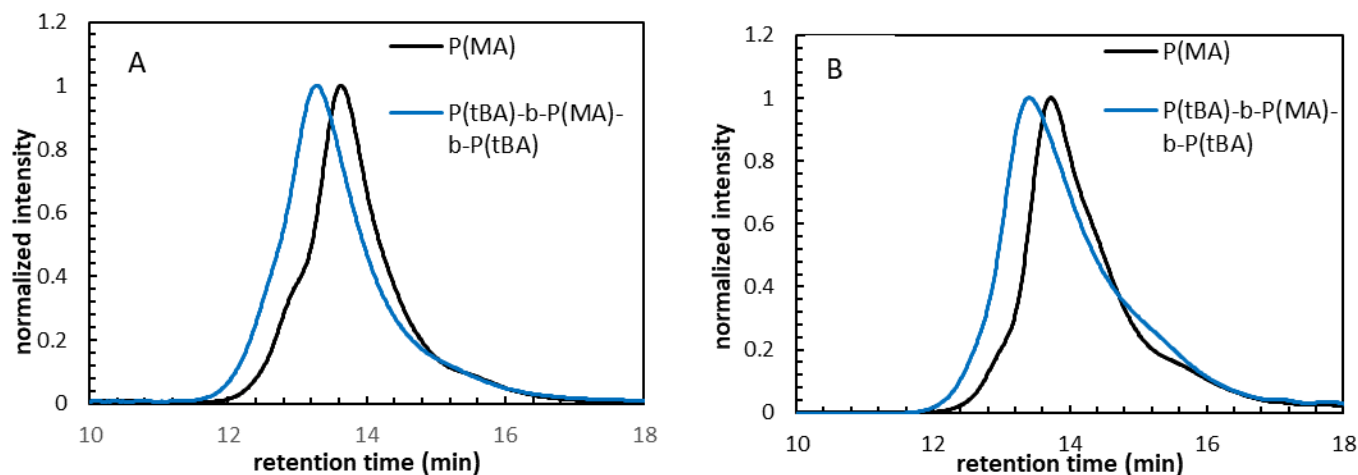
and 9 depict a disappearance of the vinyl peaks in the range of 5.5-6.5 ppm and the appearance of the methyl peak at 1.44 ppm after purification, indicating that tBA was added to P(MA).



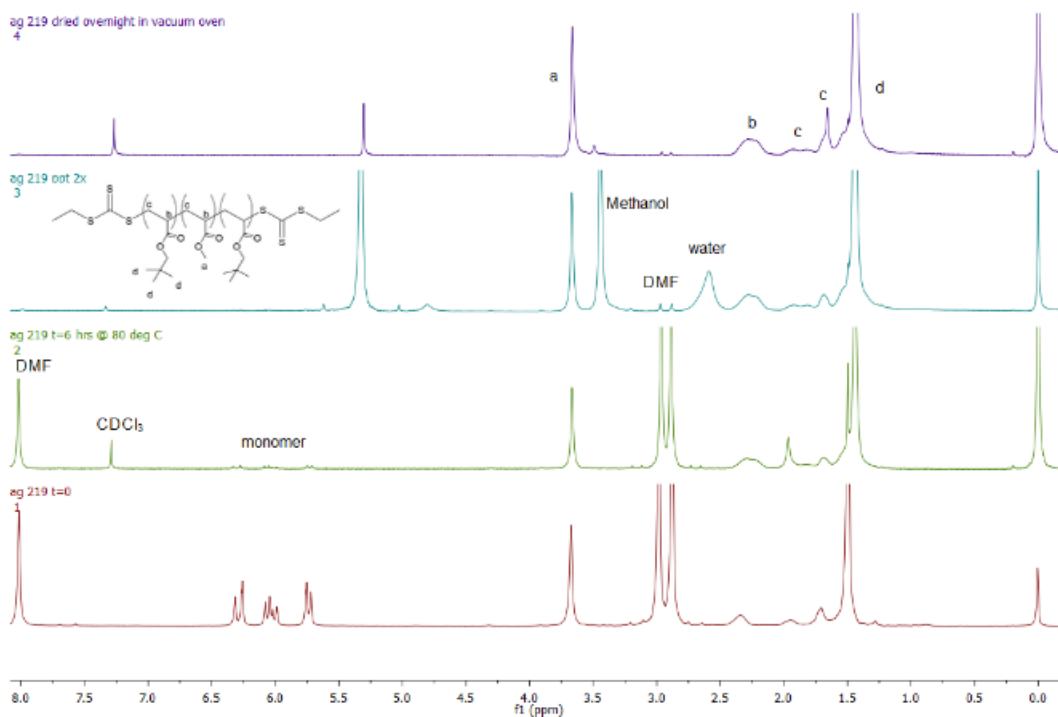
**Scheme 5.** Chain extension of P(MA) with tBA for 1.25 hours and 3 hours to produce polymers with an  $X_n$  of 79 and 328, respectively.



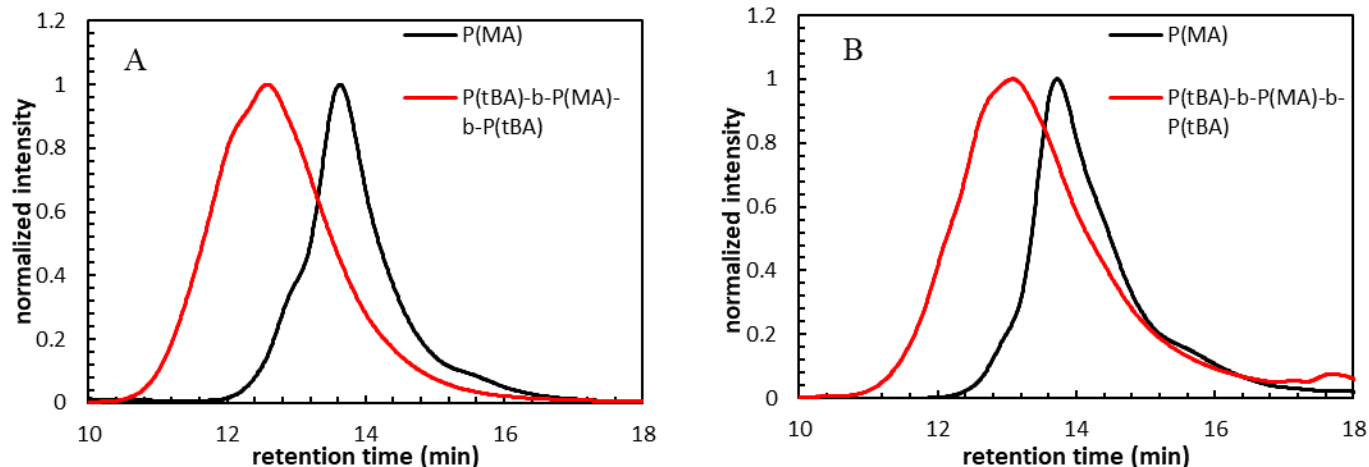
**Figure 7.** Comparative NMR spectra of the extension P78. From bottom to top: comparing starting material, after reaction time, first purification, and dried polymer.



**Figure 8.** GPC comparisons showing (A) light scattering (B) differential refractive index plots of the central P(MA) and the triblock polymer, P78.



**Figure 9.** Comparative NMR spectra of the extension of P328. From bottom to top: starting material, after reaction time, first purification, and dried polymer.



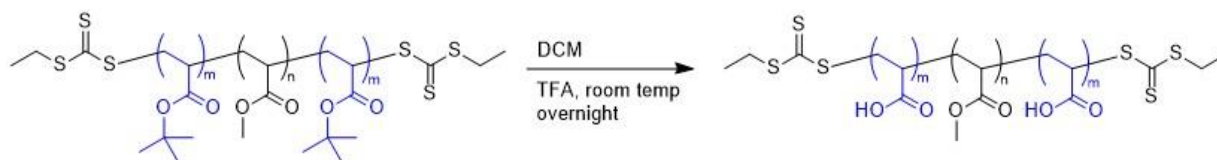
**Figure 10.** GPC comparison showing (A) light scattering (B) differential refractive index plots of the P(MA) central block to the triblock polymer, P328.

Figure 8 and Figure 10 depict a decrease in retention time indicating that the chain extension was successful. Through GPC, the  $M_n$  for the polymer with the target of 30% hydrophilic composition was calculated to be 38,500 g/mol with a dispersity of 1.23. In the second run of the same polymer through GPC, the  $M_n$  was 22,000 g/mol with a dispersity of 1.23. The polymer with the target of 70% hydrophilic composition was calculated to be 52,000 g/mol with a dispersity of 1.35. In the second run of the same polymer through GPC, the  $M_n$  was 42,000 with a dispersity of 1.47. Because of the difference of  $M_n$  between the two GPC runs, it was decided to use NMR to calculate the  $M_n$ . Through NMR, the  $M_n$  for the polymer with the target of 30% hydrophilic composition was calculated to be 28,000 g/mol. After subtracting the  $M_n$  of P(MA) the percent hydrophilic composition was calculated to be 24%. The polymer with the target of 70% hydrophilic composition was calculated to be 60,000 g/mol. After subtracting the  $M_n$  of P(MA) the percent hydrophilic composition was calculated to be 57%. Using the NMR calculated  $M_n$ , the degree of polymerization ( $X_n$ ) for the polymer with 24% hydrophilic composition was calculated to be 78 and will be referred to as P78. For the polymer with 57%

hydrophilic composition the  $X_n$  was calculated to be 328 and will be referred to as P328. Both polymers have the same  $X_n$  for the hydrophobic block which was calculated to be 205.

### 3.3 Removal of t-butyl group

After the chain extension was performed, the t-butyl group was removed to convert tBA to acrylic acid (AA) through hydrolysis. The  $^1\text{H}$  NMR spectra on Figure 11 and 12 shows the removal of the t-butyl group as confirmed by the disappearance of the characteristic t-butyl peak at 1.44 ppm, and the appearance of the hydroxyl group. The yield of P328 was 87% and the yield of P78 was 86% after the removal of the t-butyl group.



**Scheme 6.** Removal of t-butyl group through hydrolysis to form P(AA)-*b*-P(MA)-*b*-P(AA).

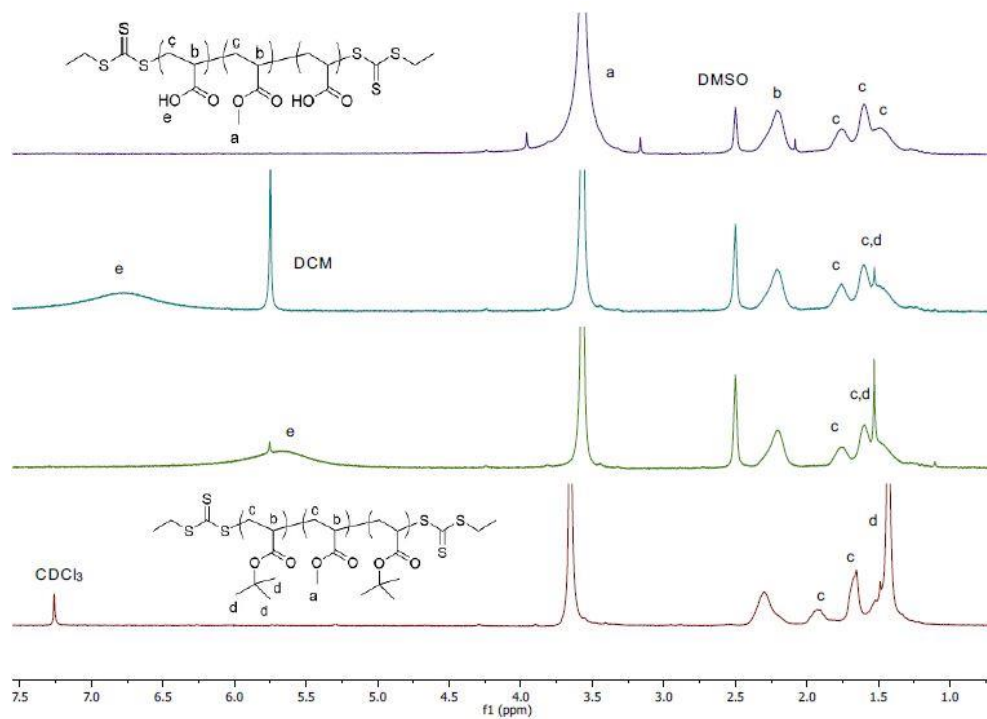


**Figure 11.** Comparative NMR spectra after t-butyl removal of P78. From bottom to top: starting material of P(tBA)-b-P(MA)-b-P(tBA), second hydrolysis, purification, and dried P(AA)-b-P(MA)-b-P(AA).

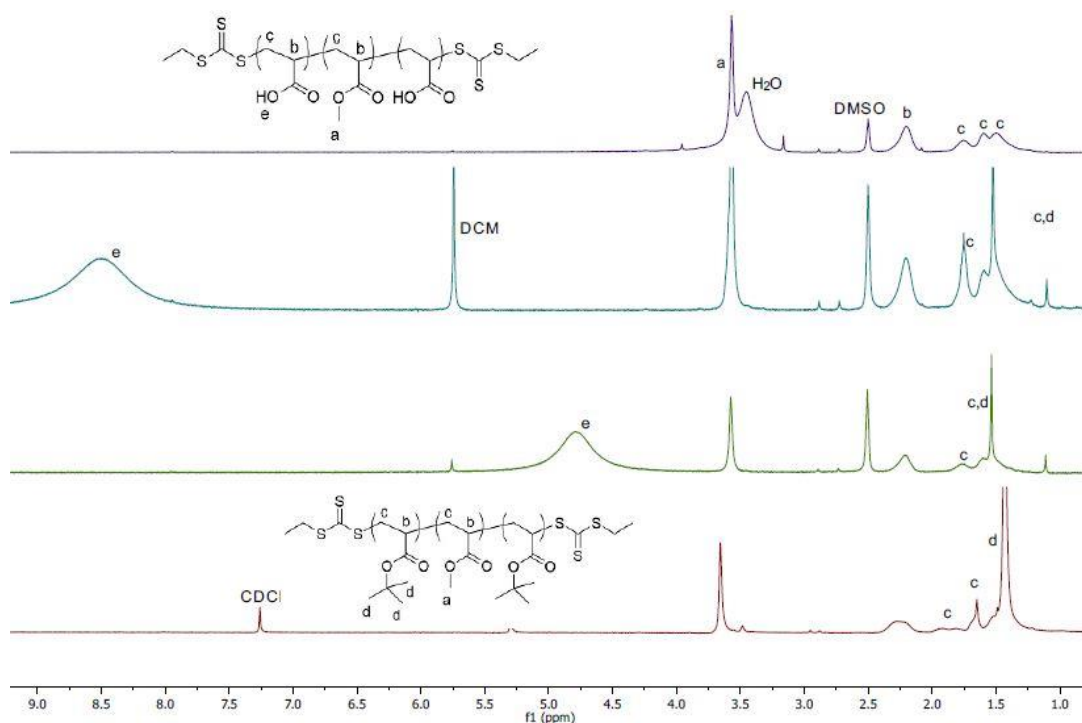


**Figure 12.** Comparative NMR spectra after t-butyl removal from P328. From bottom to top starting material of P(tBA)-*b*-P(MA)-*b*-P(tBA), second hydrolysis, purification, and P(AA)-*b*-P(MA)-*b*-P(AA).

### 3.4 Self- and co-assembly of P78 and P328

P78 and P328 were first self-assembled separately and then mixed at the following ratios (P78: P328): 25:75, 50:50, and 75:25. The morphologies obtained from the self- and co-assembly of the polymers were characterized by DLS and SLS. DLS was used to determine the hydrodynamic radius ( $R_h$ ) and SLS was used to determine the radius of gyration ( $R_g$ ). The unfiltered samples will be the primary focus because it is an accurate representation of the assembly process. The filtered samples were used to determine if the size of the assembly morphologies could be controlled.

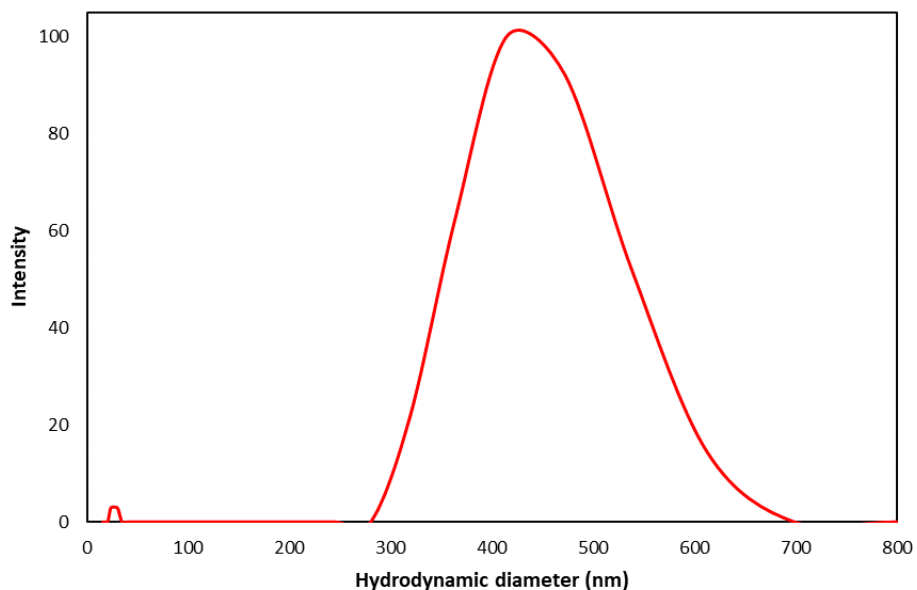


**Figure 13.** Hydrodynamic diameter distribution curve of the morphologies obtained from the self-assembly of P78 triblock at 90°.

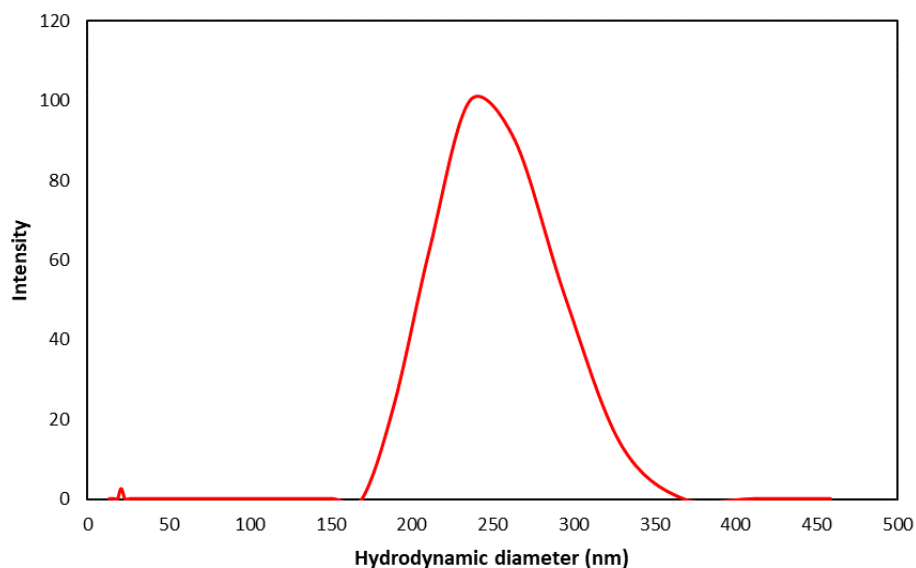


**Figure 14.** Hydrodynamic diameter distribution curve of the morphologies obtained from P328 triblock at 90°.

The  $R_h$  values for the morphologies obtained from the self-assembly of P78 and P328 were 123 and 74 nm, respectively based on multiangle DLS. This suggests that P78, triblock with a smaller hydrophilic block, self-assembled into larger morphologies whereas P328,

triblock with a larger hydrophilic block, self-assembled into smaller morphologies. Figures 13 and 14 represent the distribution curves for the hydrodynamic diameter of the morphologies obtained from the self-assembly of P78 and P328, respectively. In Figure 13, the distribution curve is in the range of 300-700 nm hydrodynamic diameter whereas, in Figure 14, the distribution curve is in the range of 175-375 nm hydrodynamic diameter.

The radius of gyration ( $R_g$ ) for P328 was 211 nm. The ratio of  $R_g/R_h$  can be used to determine the morphology of the co-assembled polymer.<sup>17</sup> When  $R_g/R_h$  ratio is less than one, the expected structure is a micelle. If the ratio equals to one, the expected structure is a vesicle. If the ratio is greater than one, the expected structure is a cylindrical micelle. For P328, the  $R_g/R_h$  ratio was 2.85 which suggests that structure is a cylindrical micelle.

**Table 1.** Light scattering data for the unfiltered samples

Sample	Hydrodynamic Radius ( $R_h$ ) (nm)
100:0	123
25:75	420
50:50	102
75:25	115
0:100	74

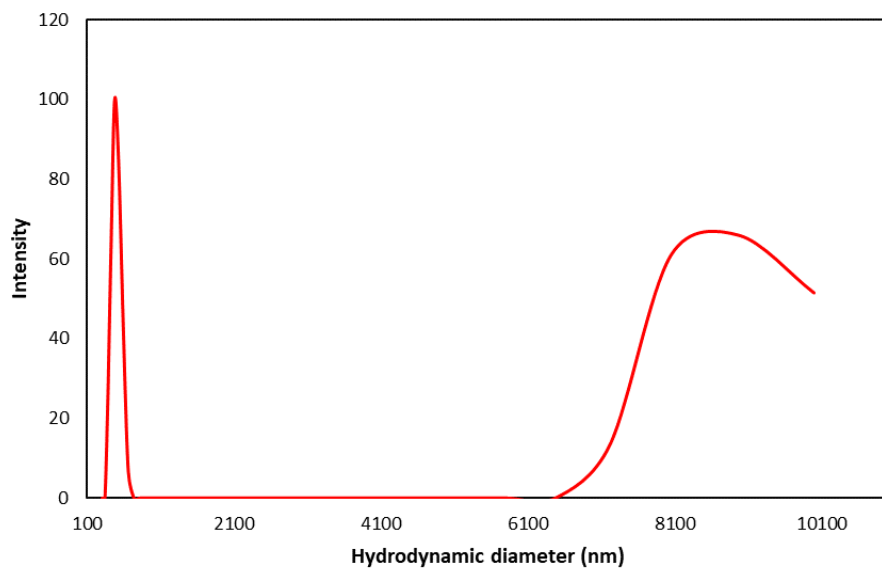


**Figure 15.** Hydrodynamic diameter distribution curve of the morphologies obtained from the 25:75 (P78:328) mixture co-assembly 90°.

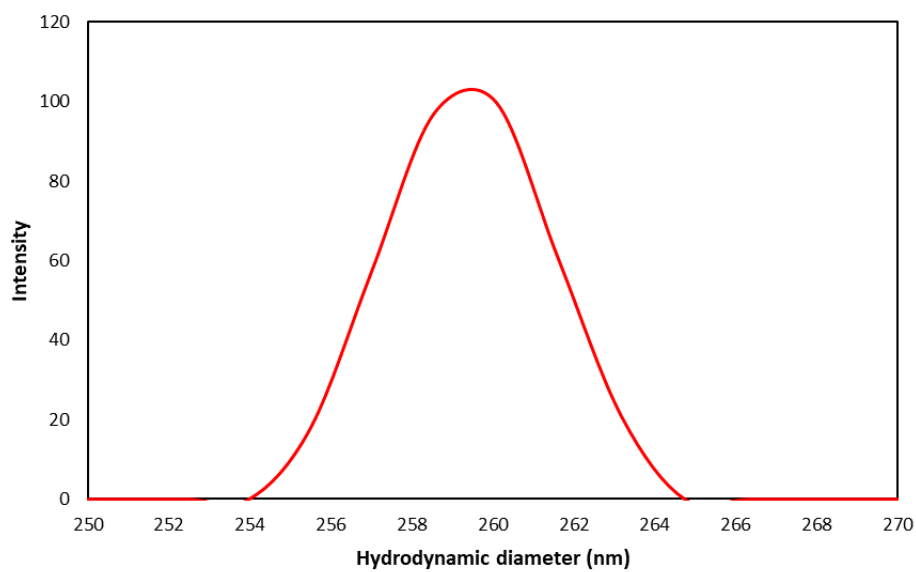


**Figure 16.** Hydrodynamic diameter distribution curve of the morphologies obtained from the 50:50 (P78:P328) mixture co-assembly 90°.

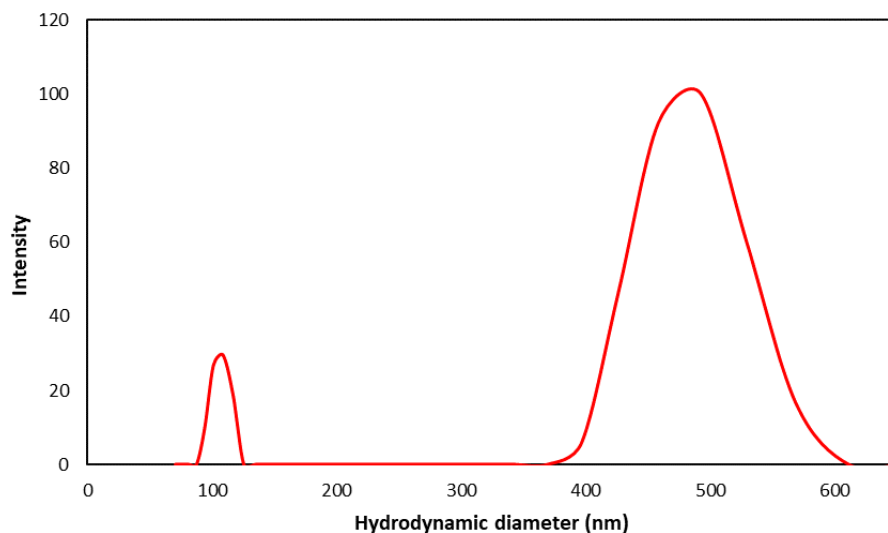


**Figure 17.** Hydrodynamic diameter distribution curve of the morphologies obtained from the 75:25 (P78:P328) mixture co-assembly 90°.

Table 1 displays the  $R_h$  values of the morphologies obtained from the co-assembly of the triblocks. In the 25:75 co-assembly, Figure 15 depicts that there are two distributions. This suggests that there are two particle sizes that fall in the 350-750 and 6,500-10,000 nm range. However, the 6,500-10,000 nm curve is more predominant than the other curve, suggesting that majority of the particles' hydrodynamic diameter fall within this range. In the 50:50 co-assembly, Figure 16 illustrates only one distribution curve, suggesting that there is one particle size and that it falls in the range of 250-265 nm. In the 75:25 co-assembly, Figure 17 depicts that there are two distribution curves. This suggests that there are two particle sizes which fall in the 75-125 and 400-600 nm range. However, the 400-600 nm curve is more predominant than the other curve, suggesting that majority of the particles' hydrodynamic diameter fall within this range. Comparing the hydrodynamic diameter of 25:75 (P78:P328) and the 75:25 (P78:P328), we get a bigger diameter size from the 25:75 and a smaller diameter size for the 75:25. This could be because P328 has a larger hydrophilic block than P78 and is expected to produce large particle sizes.

As Figure A-1 shows, no useful information could be obtained from the Zimm plot from the co-assembly of the 50:50 mixture of P78:P328. The SLS data will be further studied in the future to understand the variation in the data. To investigate what is occurring during the co-assembly, transmission electron microscopy (TEM) could be used to visually analyze the morphologies of the co-assembled triblocks.

**Table 2.** Comparison of the hydrodynamic radius of the unfiltered and filtered samples.

Sample (P78:P328)	Hydrodynamic Radius ( <i>R<sub>h</sub></i> ) (nm)	
	Unfiltered	Filtered
100:0	123	66
25:75	420	71
1:1	102	87
75:25	115	80
0:100	74	64

The filtered samples had a smaller particle size than the unfiltered samples as the values are represented in Table 2. The filtered samples had a lower turbidity than the unfiltered samples. This could be that filtration trapped majority of the polymer. In future, this could be investigated by TEM to visually compare the morphologies of the unfiltered samples to the filtered samples.

## **Chapter 4**

### **Conclusion**

In this project, two amphiphilic triblock polymers with different hydrophilic block lengths were synthesized and assembled in aqueous solution. DLS and SLS were used to characterize the morphologies of the triblocks co-assembled in different ratios. The unfiltered samples had larger hydrodynamic radii than that of the filtered samples. When the triblocks were co-assembled in a one-to-one ratio, a single distribution curve of the hydrodynamic diameter was observed. However, when one triblock content dominated the other, two distribution curves were observed. Conclusive SLS data was unable to be collected for the self-assembled morphologies of P78 and for the co-assembled morphologies since the scattered light intensity could not be measured. Future investigations could include further characterization of the unfiltered samples via TEM in order to visually analyze the morphologies of the co-assembled polymers. Another characterization method that could be done is to add fluorescence resonance electron transfer (FRET) pairs and use fluorescence microscopy to determine if co-assembly occurred.

## Reference

1. Ian, W.; GuoJun, L., Self-assembly and chemical processing of block copolymers: a roadmap towards a diverse array of block copolymer nanostructures. *Science China Life Sciences* **2013**.
2. Mai, Y.; Eisenberg, A., Self-assembly of block copolymers. *Chem Soc Rev* **2012**, *41* (18), 5969-85.
3. Feng, H.; Lu, X.; Wang, W.; Kang, N. G.; Mays, J. W., Block Copolymers: Synthesis, Self-Assembly, and Applications. *Polymers (Basel)* **2017**, *9* (10).
4. Schacher, F. H.; Rugar, P. A.; Manners, I., Functional Block Copolymers: Nanostructured Materials with Emerging Applications. *Angewandte Chemie International Edition* **2012**, *51* (32), 7898-7921.
5. Lodge, T. P., Block Copolymers: Past Successes and Future Challenges. *Macromolecular Chemistry and Physics* **2003**, *204* (2), 265-273.
6. Guo, X.; Choi, B.; Feng, A.; Thang, S. H., Polymer Synthesis with More Than One Form of Living Polymerization Method. *Macromolecular Rapid Communications* **2018**, *39* (20), 1800479.
7. Grubbs, R. B.; Grubbs, R. H., 50th Anniversary Perspective: Living Polymerization—Emphasizing the Molecule in Macromolecules. *Macromolecules* **2017**, *50* (18), 6979-6997.
8. Matyjaszewski, K.; American Chemical Society. Division of Polymer Chemistry.; American Chemical Society. Meeting, *Controlled radical polymerization*. American Chemical Society: Washington, DC, 1998; p xii, 483 p.
9. Shipp, D., Reversible-Deactivation Radical Polymerizations. *Polymer Reviews* **2011**, *51*, 99-103.
10. Boyer, C.; Bulmus, V.; Davis, T. P.; Ladmiral, V.; Liu, J.; Perrier, S., Bioapplications of RAFT Polymerization. *Chemical Reviews* **2009**, *109* (11), 5402-5436.
11. Radical Chain Polymerization. *Principles of Polymerization* **2004**, 198-349.
12. Chiefari, J.; Mayadunne, R. T. A.; Moad, C. L.; Moad, G.; Rizzardo, E.; Postma, A.; Thang, S. H., Thiocarbonylthio Compounds (SC(Z)S-R) in Free Radical Polymerization with Reversible Addition-

Fragmentation Chain Transfer (RAFT Polymerization). Effect of the Activating Group Z.

*Macromolecules* **2003**, *36* (7), 2273-2283.

13. Moad, G.; Chong, Y. K.; Postma, A.; Rizzardo, E.; Thang, S. H., Advances in RAFT polymerization: the synthesis of polymers with defined end-groups. *Polymer* **2005**, *46* (19), 8458-8468.

14. Chong, Y. K.; Krstina, J.; Le, T. P. T.; Moad, G.; Postma, A.; Rizzardo, E.; Thang, S. H., Thiocarbonylthio Compounds [SC(Ph)S-R] in Free Radical Polymerization with Reversible Addition-Fragmentation Chain Transfer (RAFT Polymerization). Role of the Free-Radical Leaving Group (R). *Macromolecules* **2003**, *36* (7), 2256-2272.

15. Darling, S., Directing the self-assembly of block copolymers. *Prog. Polym. Sci.* **32**(10), 1152-1204. *Progress in Polymer Science - PROG POLYM SCI* **2007**, *32*, 1152-1204.

16. Blanazs, A.; Armes, S. P.; Ryan, A. J., Self-Assembled Block Copolymer Aggregates: From Micelles to Vesicles and their Biological Applications. *Macromol Rapid Commun* **2009**, *30* (4-5), 267-77.

17. Patterson, J. P.; Robin, M. P.; Chassenieux, C.; Colombani, O.; O'Reilly, R. K., The analysis of solution self-assembled polymeric nanomaterials. *Chemical Society Reviews* **2014**, *43* (8), 2412-2425.

18. Aragón, S.; Pecora, R., Theory of dynamic light scattering from polydisperse systems. *The Journal of Chemical Physics* **1976**, *64*, 2395-2404.

19. Anderson, D. J.; Guo, B.; Xu, Y.; Ng, L. M.; Kricka, L. J.; Skogerboe, K. J.; Hage, D. S.; Schoeff, L.; Wang, J.; Sokoll, L. J.; Chan, D. W.; Ward, K. M.; Davis, K. A., Clinical Chemistry. *Analytical Chemistry* **1997**, *69* (12), 165-230.

20. Technology: Dynamic Light Scattering (DLS) - Introduction.

<https://lsinstruments.ch/en/technology/dynamic-light-scattering-dls> (accessed November 14).

21. Zimm, B. H., Apparatus and Methods for Measurement and Interpretation of the Angular Variation of Light Scattering; Preliminary Results on Polystyrene Solutions. *The Journal of Chemical Physics* **1948**, *16* (12), 1099-1116.

22. Technology: Static Light Scattering (SLS) - Introduction.

<https://lsinstruments.ch/en/technology/static-light-scattering-sls> (accessed November 14).

23. York, A. W.; Kirkland, S. E.; McCormick, C. L., Advances in the synthesis of amphiphilic block copolymers via RAFT polymerization: Stimuli-responsive drug and gene delivery. *Advanced Drug Delivery Reviews* **2008**, *60* (9), 1018-1036.

## Appendix

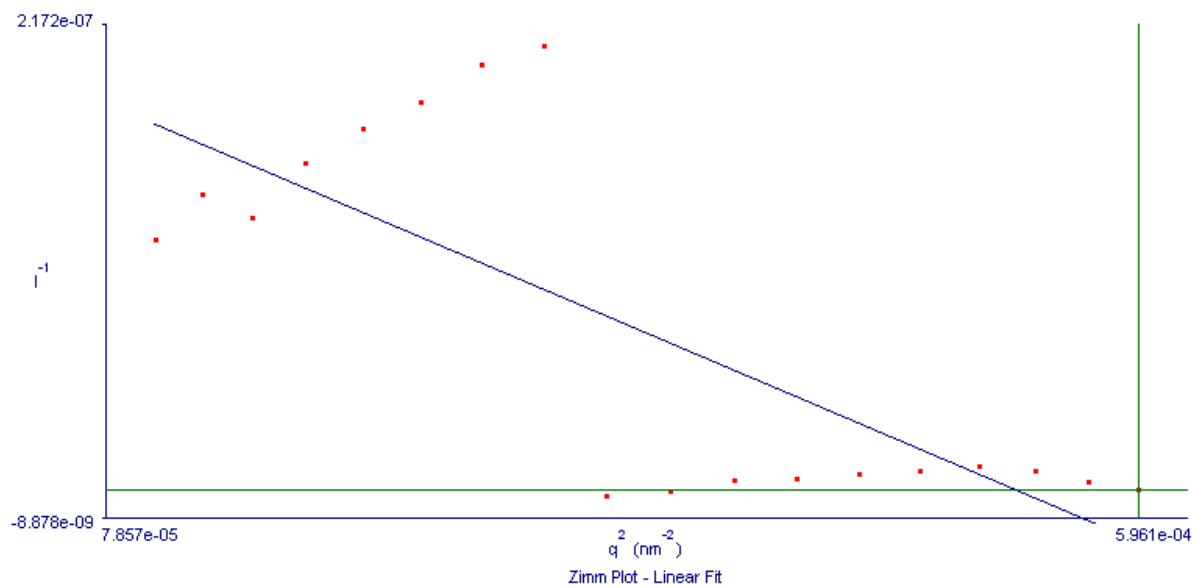


**Figure A-1.** The Zimm plot from the co-assembly of the 50:50 mixture of P78:P328.